The Meteoritical Society

Meteoritics & Planetary Science 47, Nr 5, 820–831 (2012)
doi: 10.1111/j.1945-5100.2012.01355.x

Synthesis of a spinifex-textured basalt as an analog to Gusev crater basalts, Mars

Nicolas BOST[1–4*], Frances WESTALL[1], Fabrice GAILLARD[2–4], Claire RAMBOZ[2–4], and Frédéric FOUCHER[1]

[1]Centre de Biophysique Moléculaire, UPR CNRS 4301, 45071, Orléans, France
[2]Univ d'Orléans, ISTO, UMR 7327, 45071, Orléans, France
[3]CNRS/INSU, ISTO, UMR 7327, 45071 Orléans, France
[4]BRGM, ISTO, UMR 7327, BP 36009, 45060 Orléans, France
[*]Corresponding author. E-mail: nicolas.bost@cnrs-orleans.fr.

(Received 15 December 2011; revision accepted 17 March 2012)

Abstract–Analyses by the Mars Exploration Rover (MER), Spirit, of Martian basalts from Gusev crater show that they are chemically very different from terrestrial basalts, being characterized in particular by high Mg- and Fe-contents. To provide suitable analog basalts for the International Space Analogue Rockstore (ISAR), a collection of analog rocks and minerals for preparing in situ space missions, especially, the upcoming Mars mission MSL-2011 and the future international Mars-2018 mission, it is necessary to synthesize Martian basalts. The aim of this study was therefore to synthesize Martian basalt analogs to the Gusev crater basalts, based on the geochemical data from the MER rover Spirit. We present the results of two experiments, one producing a quench-cooled basalt (< 1 h) and one producing a more slowly cooled basalt (1 day). Pyroxene and olivine textures produced in the more slowly cooled basalt were surprisingly similar to spinifex textures in komatiites, a volcanic rock type very common on the early Earth. These kinds of ultramafic rocks and their associated alteration products may have important astrobiological implications when associated with aqueous environments. Such rocks could provide habitats for chemolithotrophic microorganisms, while the glass and phyllosilicate derivatives can fix organic compounds.

INTRODUCTION

In situ missions to planetary surfaces benefit from testing payload instruments with the same suite of materials. Within this context, we are constructing a collection of planetary analog rocks: the International Space Analogue Rockstore (ISAR, Bost et al. 2011) for testing in situ instrumentation. ISAR is accompanied by a database of the relevant information about the rock and mineral samples available (www.isar.cnrs-orleans.fr). In view of the actual and upcoming missions to Mars, Mars Science Laboratory and the International 2018 Mission, our collection of analog materials is primarily centered around Martian rock analogs including igneous rocks (basalts, cumulates), sediments (volcanic, hydrothermal), and minerals (phyllosilicates, carbonates, sulfates, etc.). Basalts are particularly important to the ISAR collection because they are dominant on Mars (e.g., McSween et al. 2009).

Based on analyses of SNC Martian meteorites and on in situ analyses on Mars during the Pathfinder and MER missions, the composition of Martian basalts varies depending upon the materials and/or the analytical methods used. In Fig. 1, the total alkali-content (TAS) and FeO*/MgO ratios of Martian basaltic rocks are plotted as a function of wt% SiO_2 (Figs. 1a and 1b, respectively; [Economou 2001; Gellert et al. 2006; Ming et al. 2008; McSween et al. 2009]). Figures 1a and 1b show that most in situ measurements plot within the basaltic field, whereas SNC meteorites plot outside it within the komatiite field (hatched area, Fig. 1a). Shergottites have lower alkali- and lower Fe- and Mg-contents than basaltic rocks, while nakhlites are richer in SiO_2 than basalts. This is probably due to the fact that SNC meteorites are cumulate-type facies rather than basalt melts (McSween et al. 2009). Most terrestrial volcanic rocks from the ISAR collection are basalts; however, all of them plot outside the Martian field in the FeO*/MgO versus SiO_2 diagram (Fig. 1b), as well as in the TAS diagram (except for one "picritic" basalt from Etna, sample 09ET01, Fig. 1a). Terrestrial basalts are

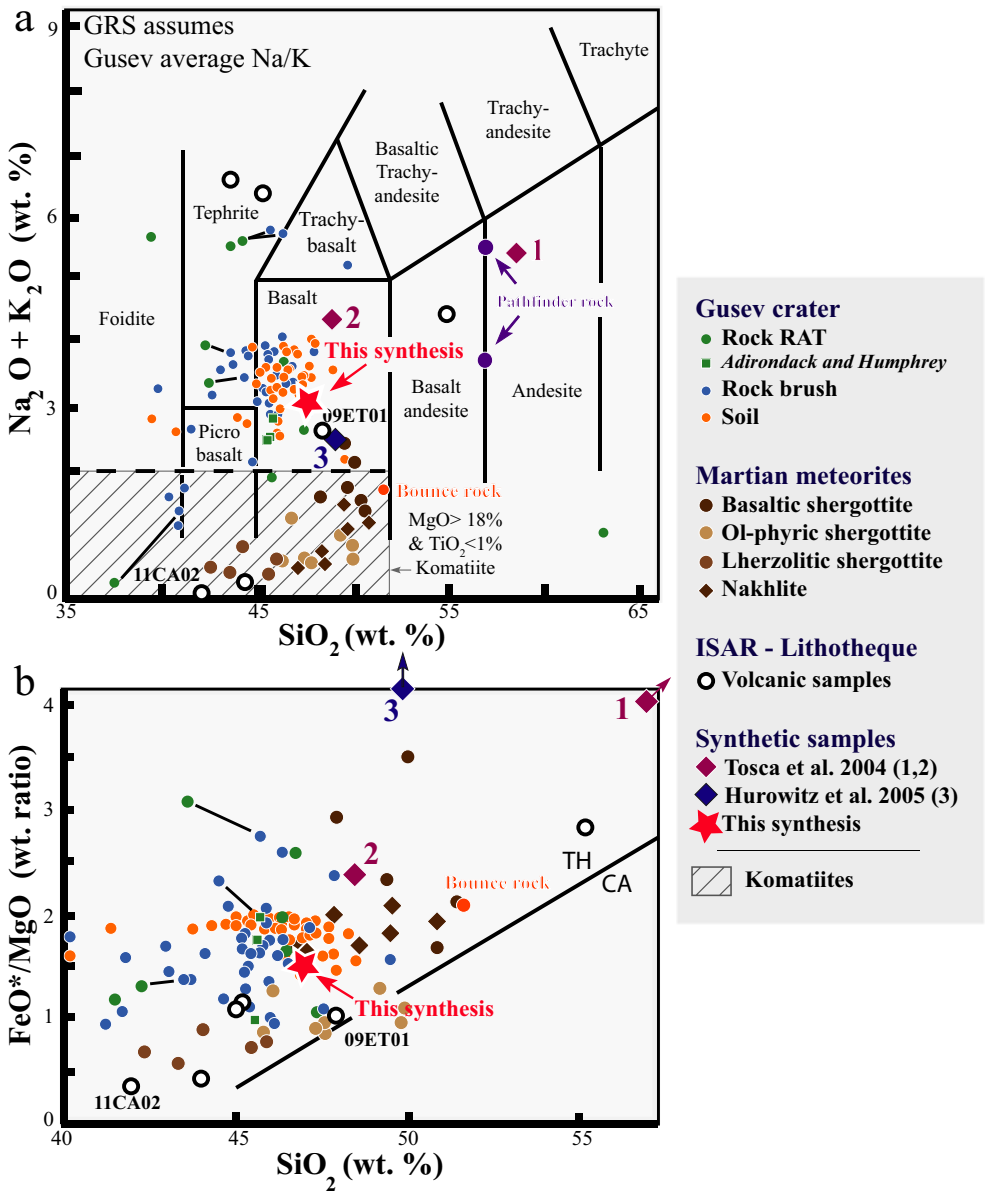

Fig. 1. $Na_2O + K_2O$ oxides and FeO*/MgO ratios versus SiO_2 plots (in wt%; a and b, respectively): composition of our synthetic basalt (red star) as compared to that of in situ Martian basalts and SNC Martian meteorites (after McSween et al. 2009; Le Bas 2000). The terrestrial volcanic samples presently included in the ISAR lithotheque are also shown (black circles; sample names after Bost et al. 2011). The synthetic Pathfinder rock (1) and soil (2) from Tosca et al. (2004) and the synthetic Los Angeles sample (3) from Hurowitz et al. (2005) are also shown for comparison. The Bounce rock is the only sample of basaltic origin that was analyzed in the Meridiani Planum by the Opportunity rover (Rieder et al. 2004; Zipfel et al. 2004). The FeO*/MgO-silica diagram is used for distinguishing dry tholeiitic (TH) and wet calc-alkaline (CA) rocks. All Martian samples are tholeiitic.

notably Fe-Mg poorer than Martian rocks (McSween et al. 2009). This is the reason why it is necessary to synthesize Martian basalts for testing payload instruments, as well as for analog laboratory experiments.

Previous attempts have been made to create artificial Martian basalts. Tosca et al. (2004) based their synthesis on data from the APX Spectrometer on the Sojourner rover reported by Economou (2001); Wänke et al. (2001). Plotted in the TAS diagram in Fig. 1a, the latter in situ analyses are richer in silica and have a more andesitic composition than those made by the rover Spirit in Gusev crater. This is because the Pathfinder rock surfaces were not cleaned before analysis and what was analyzed was a silica-rich weathered rind (McSween et al. 2009). Recent

Table 1. Chemical analyses of rough and abraded surfaces using the RAT tool, obtained on Mars in Gusev crater by the MER Spirit (after Gellert et al. 2006). The ration Fe^{3+}/FeT is from Morris et al. (2006) at the correspondent soil.

Oxides, wt%	Adirondack	Humphrey		Mazatzal Brooklyn	Pot of Gold	Wooly Patch		Clovis Plano	Ebenezer	Uchben Koolik
		RAT1	*RAT2*	*RAT2*		*Sabre RAT*	*Mastodon RAT*			
Soil n°	34	59	60	86 (84)	172 (171)	197 (198)	199 (200)	218	232 (233)	287
SiO_2	45.7	46.3	45.9	45.8	42.9	46.8	46.4	42.2	47.4	45.6
TiO_2	0.48	0.58	0.55	0.59	0.77	0.94	0.91	0.84	0.79	0.8
Al_2O_3	10.87	10.78	10.68	10.7	10.32	12.6	10.34	8.95	9.28	9.52
MnO	0.41	0.41	0.41	0.42	0.24	0.1	0.13	0.3	0.16	0.25
MgO	10.83	9.49	10.41	9.72	9.91	10.92	11.62	11.52	14.82	14.28
CaO	7.75	8.19	7.84	8.02	5.86	3.64	3.44	6.04	3.44	4.48
Na_2O	2.4	2.8	2.5	2.8	3	3.3	2.9	3.6	2.3	2.4
K_2O	0.07	0.13	0.1	0.16	0.2	0.07	0.04	0.35	0.33	0.35
P_2O_5	0.52	0.57	0.56	0.65	1.08	1.24	1.2	1.05	0.97	0.94
Cr_2O_3	0.61	0.68	0.6	0.54	0.27	0.27	0.18	0.17	0.16	0.15
Cl	0.2	0.32	0.26	0.23	0.57	0.78	1.03	1.63	1.46	1.85
SO_3	1.23	1.09	1.28	1.48	7.96	2.87	2.41	7.53	3.2	5.26
FeOb	18.8	18.6	18.8	18.9	16.7	16.3	19.2	15.6	15.6	13.9
Total	99.87	99.94	99.89	100.01	99.78	99.83	99.8	99.78	99.91	99.78
Fe^{3+}/Fe_T	0.16	0.19	0.15	0.10	0.51	0.59	0.61	0.84	0.83	0.79

measurements obtained in situ by Spirit (Gellert et al. 2006) show that the volcanic rocks are much closer to basalts or picro-basalts (Fig. 1a). The soil sample synthesized by Tosca et al. (2004) has a chemical composition that is more representative of Martian basalts. A second attempt to synthesize Martian rocks was made by Hurowitz et al. (2005), who used the Martian meteorite Los Angeles (described by Rubin et al. 2000) as a reference. Although this synthetic Martian basalt falls within the basalt field of the TAS diagram (Fig. 1a), its Fe and Mg composition is much higher than that of the Martian basalts analyzed in situ.

We have synthesized Martian basalts using an average composition of the basalts analyzed in situ by the MER Spirit in the Gusev crater on Mars, corrected for alteration. We produced two types of basalts, a glassy basalt that was quench cooled and a coarser grained basalt that was cooled more slowly. The spinifex textures produced in the more slowly cooled basalt were surprisingly similar to those of a volcanic rock type very common on the early Earth, the komatiites. These rock types and their alteration products are of astrobiological interest. Prebiotic organics important for the origin of life can be concentrated in clays produced by the alteration of the rocks. Also, when associated with water, the vitreous surfaces of these ultramafic rocks are ideal habitats for chemolithotrophic microorganisms that extract their essential nutrients from the rocks (P, Fe, Mg, Ni, Mn) and obtain their energy from redox reactions at their surfaces (e.g., Furnes et al. 2007; Cavalazzi et al. 2011).

MATERIALS AND METHODS

Reference Data

We based the composition of our synthetic Martian basalts on the in situ geochemical measurements made by the rover Spirit in Gusev crater. This crater is located at 14°35′S, 175°25′E and has a diameter of 166 km. The age of its volcanic rocks has been estimated to be older than 3.5 Ga (Late Noachian/Early Hesperian [Squyres et al. 2004]). We chose the Gusev data rather than the Meridiani Planum data as our reference because the materials at the Opportunity landing site are too altered to be considered as primary basalts, with the exception of the Bounce Rock, which is a shergottite-like rock (Fig. 1; Rieder et al. 2004; Zipfel et al. 2004).

Reconstruction of a Pristine Basaltic Composition

The geochemical Martian basalt analyses plotted in Fig. 1 are taken from Gellert et al. (2006). These authors analyzed the data obtained from rough, brushed (brush), and abraded (RAT) rock surfaces. Our goal was to determine a chemical composition similar to that of a fresh unaltered Martian basalt. We therefore narrowed our choice to rock analyses obtained from surfaces that had been abraded by the Rock Abrasive Tool (RAT, Table 1). However, even in the case of surfaces abraded to a depth of a few millimeters, alteration is still present, as indicated by their friability and the presence of secondary minerals (cf. McAdam et al. 2008; Viles et al. 2010 and citations therein). In correcting for the

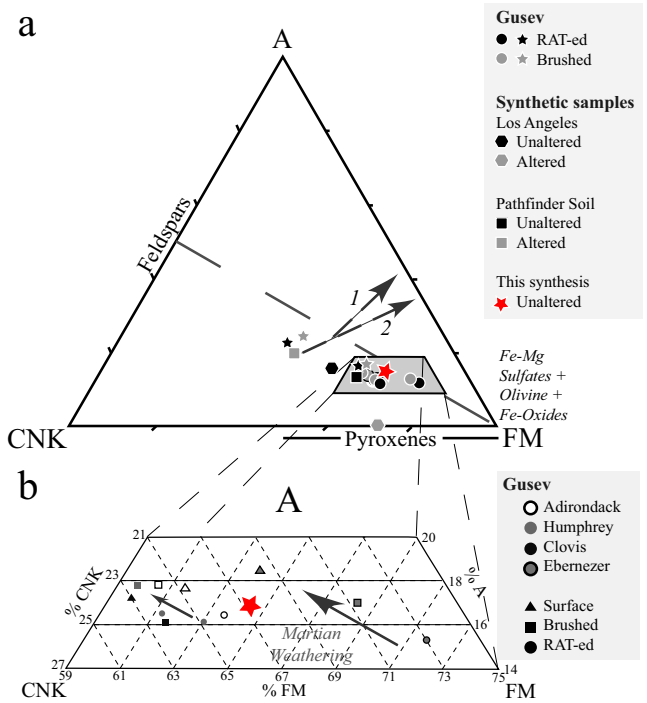

Fig. 2. a) Ternary diagram of total (mole%) FeO* + MgO (FM), Al_2O_3 (A), CaO + Na_2O + K_2O (CNK) showing the chemical evolution of basaltic rocks during terrestrial weathering (dotted arrows: Baynton basalt, Australia (1) and basaltic samples described by Nesbit and Wilson (1992), plus Deccan basalt (2) weathering products by Greenberger et al. 2011) compared to the rocks analyzed in the Gusev crater on Mars by Spirit and two synthetic samples (square, Tosca et al. 2004; hexagon, Hurowitz et al. 2005). Note the two directions of alteration of rocks in Gusev crater (circles and stars). We consider that Wishstone, Champagne, and Watchtower (stars) are marginal and that Adirondach, Humphrey, Ebenezer, and Clovis (circles; Table 1; by Hurowitz et al. 2006) are representative samples. The samples from this study correspond to the red stars. b) Enlarged plot of the box in (a) showing the Martian weathering effect (full arrow). Whatever the composition of the basalt, weathering induces a drastic loss of MgO and FeO with a slight variation of Al_2O_3 and CaO + Na_2O + K_2O. Hurowitz et al. (2006) show that the effects of weathering seem to be different on Earth and on Mars (a and b, respectively).

alteration at the surface of Mars, we took into account the results of experimental alteration of Martian analog basalts (Fig. 2a; Tosca et al. 2004; Hurowitz et al. 2005). Hurowitz et al. (2005) synthesized a shergottite with a gabbroic texture using the Los Angeles meteorite as a starting composition. The alteration of the material under Martian conditions resulted in a large decrease in Al_2O_3 and a slight increase in FeO and MgO (Fig. 2b). This type of alteration was probably favored by the holocrystalline texture of the rock characterized by a porphyritic texture dominated by large, easily alterable plagioclase laths. On the other hand, the basaltic (olivine-rich) soil used by Tosca et al. (2004) documented a significant decrease in the FeO- and MgO-content with alteration, and a slight increase in CaO, Na_2O, and K_2O, with alteration but more or less stable Al_2O_3 contents (Figs. 2a and 2b). Another study based on the in situ Martian MER analyses by Hurowitz et al. (2006) shows an alteration process that follows the trend experimentally produced by Tosca et al. (2004) with the preferential dissolution of olivine in low pH conditions.

Geochemical Composition of the Samples

The chemical composition of our artificial Martian basalt was based on the average composition of the ten most similar analyses of RAT-abraded Gusev basalts (Table 2, Fig. 1; Gellert et al. 2006). The ten selected analyses show little variability in their weight percentages of oxides. We chose Adirondack, Humphrey and Mazatzal Brooklyn because they are certainly the least altered basalts. The other basalts show varying degrees of alteration, even on the RATted surfaces. Pot-of-Gold and Woolly Patch are less altered than Clovis, Ebernezer, and Uchben (Morris et al. 2006). We therefore corrected for the alteration by choosing a basalt composition that has no volatiles (also because fluid basalts extruded at the surface of Mars were more likely to be degassed). Thus, we did not include volatile elements, such as Cl, S, C, or water, for this synthesis even though Gaillard and Scaillet (2009) have shown that degassed Martian basalts can retain ca. 0.1 wt% S. We also increased the Fe and Mg contents. Al was also not increased to take into account the Al_2O_3 reaction.

Thus, as shown in Fig. 1, our average composition is in complete agreement with the elemental composition of the Martian basalts analyzed in situ, taking into account the surface alteration of the Martian rocks (McSween et al. 2009). Our bulk composition is very similar to that used in previous studies (e.g., Filiberto et al. 2008; Stanley et al. 2011). We assumed that the magma was extruded at the surface and was therefore completely degassed. No viscous rhyolitic-type lavas have yet been unambiguously observed at the surface of Mars. In our experiment, the high concentrations of Mg produce a very fluid magma. Similar Mg-rich melts that were common on the early Earth produced very thin, fluid, degassed lavas called komatiites.

Methods

The basic ingredients were provided as powdered oxides (SiO_2, TiO_2, P_2O_5, Al_2O_3, Cr_2O_3, MnO, FeO, MgO, K_2O, and NiO) except for CaO and Na_2O that were present as carbonates. The weight percent of each ingredient is reported in Table 2. Note that we used

Table 2. Compared analyses of synthetic Martian basalts (PFS: Tosca et al. 2004; SLA: Hurowitz et al. 2005), a picritic basalt from Etna (sample 09ET01 included in ISAR, Bost et al. 2011) and a synthetic basalt (this work), analog of Martian basalts from the Gusev crater (see analyses in Table 1).

Oxides, wt%	SiO_2	TiO_2	P_2O_5	Al_2O_3	Cr_2O_3	MnO	FeO	MgO	CaO	Na_2O	K_2O	NiO
PFS	48.68	1.16	1.19	10.29	–	0.49	19.23	7.66	7.07	3.56	1.02	–
SLA	49.8	1.27	0.77	10.9	–	0.43	20.4	3.34	9.7	2.32	0.26	–
09ET01	48.09	1.02	0.29	11.29	–	0.18	10.43	12.06	12.67	1.82	0.95	–
Mean (Target)	47.58	0.76	0.92	10.87	0.37	0.29	18.00	11.90	6.12	2.94	0.19	0.05

ferrous iron (FeO) at 99.5% purity in this experiment. The total amount of material used was 2g. The oxides were mixed together in an agate mortar and then placed in an open alumina crucible that was positioned in a circular vertical oven (Adamel^{TM}) at atmospheric pressure (10^5 Pa). We assumed that the surface pressure on early Mars was more or less similar to that of the Earth's surface today (Halevy et al. 2007). To obtain reducing conditions, an atmosphere of 80% CO_2 and 20% CO was used in the chamber. Such a gas mixture imposes an oxygen fugacity near FMQ -1 (i.e., 1 log unit more reducing that the oxygen fugacity buffered by the fayalite-magnetite-quartz redox buffer), which corresponds to oxidizing conditions recorded in Shergottite rocks (Herd et al. 2002). Note that higher FMQ values of FMQ-3 were determined for the later crystallization stage of NWA 1068/1110 by Herd (2006), whereas Schmidt et al. (2011) determined an FMQ between −4 and +3 for a Gusev basalt. On Mars, the average melting conditions are estimated to be between 1.0 to 1.2 GPa and between 1320 to 1550 °C (Musselwhite et al. 2006; Monders et al. 2007). In this study, the samples were heated to 1350 °C and exposed to the CO-CO_2 atmosphere for 3 h. We used Al_20_3 containers to avoid iron loss from the samples to the kind of metal containers normally used for such high temperature experiments (Gaillard et al. 2003). Previous experiments on basaltic melts at similar temperatures have shown that interactions between melt and alumina container are negligible and only a narrow region (100 μm) at the melt–alumina interface is affected (Pommier et al. 2010).

Once the melts were homogenized, the two samples were cooled at different rates. One sample was slowly cooled in the oven for one day (given the dynamics of cooling over a diameter of 2 cm, we estimate that the cooling rate was ~110 °C h^{-1}). This sample has the ISAR code 11AR01. The second sample, ISAR code 11AR02, was drop-quenched in the CO-CO_2 atmosphere from 1350 °C to room temperature. Calculation of the cooling rate in this sample shows that it reached a temperature of less than 400 °C in the core of the sample after 8 min (cooling rate > > 1400 °C h^{-1}). We thus obtained a ''crystalline'' basalt (11AR01) and a glass-rich basalt (11AR02). We did not use longer cooling times because this would have produced a gabbro-like texture, which was not our objective. Experimental study of the formation of spinifex textures in komatiites gives cooling rates between 10 °C h^{-1} and 1428 °C h^{-1} (review in Faure et al. 2006).

Once the crucibles were cold, polished sections parallel to the horizontal sample surface were made. The two polished sections were then investigated with laboratory instruments. They were observed in reflected light with an Olympus^{TM} BX51 (CNRS-CBM, Orléans, France) and then in backscattered mode with a JSM-6400 JEOL^{TM} scanning electron microscope (SEM) coupled to an EDX spectral analysis system and with a Hitachi^{TM} Tabletop TM3000 SEM (both at CNRS-ISTO, Orléans, France). Mineralogical analyses were performed using a WITec^{TM} Alpha 500 RA Raman spectrometer using a green laser light source at 532 nm as a submicrometric beam, both in scanning and in spot mode (laser power ~10 mW, CNRS-CBM). Powdered preparations of the samples were investigated using a Nicolet^{TM} Magna IR 760 spectrometer ESP associated with a NIR Nicolet^{TM} 6700 FT-IR (in reflected mode; Thermo Scientific Integration Sphere; University of Poitiers). Finally, spot elemental analyses were performed on the polished sections with a Cameca^{TM} SX-50 microprobe (ISTO-BRGM, Orléans, France). Beam conditions were 15 kV and 10 nA and the following minerals were used as standards: orthoclase (K_2O); albite (SiO_2, Na_2O); andradite (CaO, FeO); $MnTiO_3$ (MnO,TiO_2); corundum (Al_2O_3); Cr_20_3 (Cr_20_3); olivine (MgO); NiO (NiO); and apatite (P_2O_5).

RESULTS

Al–Crucible Interactions

Al-rich oxides with a normative chemical formula of $(Fe^{2+}{}_{0.24}Mg_{0.76})$ $(Fe^{3+}{}_{0.30}Cr_{0.03}Al_{1.67})$ O_4, measured using the electron microprobe, occur at the edge of the crucible to within 45 μm of the crucible walls. These spinels obviously resulted from reaction with the alumina crucible. Thus, in the following study, these reactive phases were not taken into account of the mineralogy and texture in the sample cores are described hereafter.

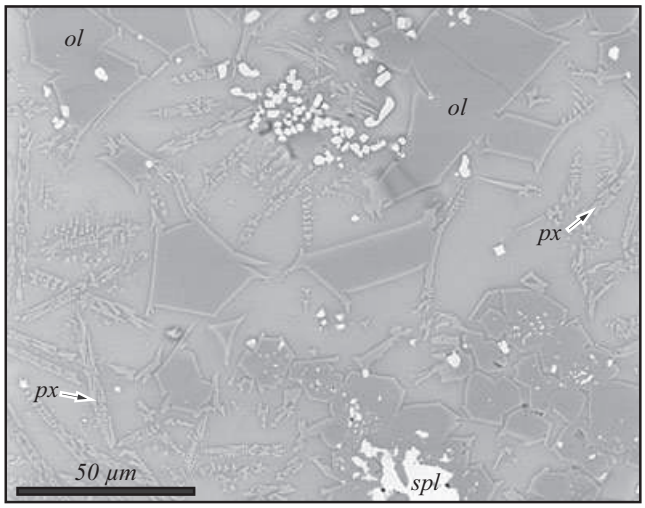

Fig. 3. Backscattered image of the inner part of sample 11AR02 (drop-quenched) in polished section. Spinels (*spl*) are in white and are associated with blocky olivine crystal (*ol-dark gray*) in a gray augitic glass containing very small dendrite crystals of pyroxenes (*px-light gray*).

Structure and Texture

Both samples exhibited an homogeneous texture in polished section, except for the fine outer reaction aureole close to the crucible. Some cracks appeared due to the retraction of the magma during cooling and crystallization. The slowly cooled basalt 11AR01 contains some rare vesicles, whereas the rapidly cooled sample (11AR02) contains many of them due to the drop quenching, which prevented out-gassing of carbonate-derived CO_2.

The drop-quenched basalt 11AR02 displays an aphanitic microlithic texture consisting of spinels, olivine crystals, and small dendritic to microlitic pyroxene crystals in a dominant glassy matrix (Fig. 3). The slowly cooled basalt 11AR01 presents different textures (Figs. 4 and 5). The pyroxenes are skeletal and very elongated and are associated with acicular olivine. This dendritic texture is similar to spinifex textures in terrestrial basalts, as shown by the comparison with an olivine spinifex-textured komatiite from Dundonald Township, Ontario (Figs. 6a and 6b, respectively; compared with Fig. 3 in Arndt et al. 2004) and from experimental study (Figs. 14a and 14b in Faure et al. 2006). The spinifex texture of this komatiite was attributed to very rapid cooling (around 1000 °C h^{-1}; Faure et al. 2006) of a melt containing very little water (only few hundred ppm H_2O; sample DUN 2 in Arndt et al. [2004], and sample 11CA02 in Bost et al. 2011). The melt conditions of our basalt were similar to those of the Dundonald komatiite in terms of very low water-content, high Mg-content, and relatively rapid cooling, although bulk chemical compositions are different (basalt versus komatiite, Fig. 1). The acicular textures observed in sample 11AR01 differ from hopper or swallow-tail-like textures observed in olivines in terrestrial submarine basalts, such as MORBs. The latter are associated with highly viscous magmas extruded at high pressure that were subjected to undercooling (Bryan 1972), a situation very different to the conditions of formation of our basalts. Our melts were cooled at a relatively rapid rate that precludes metastability (undercooling).

Mineralogy

Slowly Cooled Basalt-Sample 11AR01

The major mineralogical phases in this slowly cooled sample are large elongated clinopyroxene crystals (100×10 μm) and small olivines ($10 \times < 1$ μm) associated with spinels in a glass (Fig. 4). The probable crystallization sequence is spinel, clinopyroxene, olivine, and glass. These phases were confirmed by Raman and IR spectrometries. Microprobe analyses (Table 3) permitted more precise characterization of the large pyroxene crystals, having an average chemical formula of $(Ca_{0.21}Na_{0.07})_{\Sigma = 1 - p}$ $(Fe_{0.57}Mg_{1.02}Al_{0.12}Ti_{0.02})_{\Sigma = 1 + p}$ $(Si_{1.92}Al_{0.08})$ O_6. Their compositions range from subcalic-augite to Mg-pigeonite class. The Al-poor spinels within the basalt contrast with the Al-rich spinels formed close to the crucible walls. The average chemical composition of the basaltic spinels is $(Fe^{2+}{}_{0.51}Mg_{0.55})_{\Sigma = 1}$ $(Fe^{3+}{}_{0.63}Cr_{0.49}Al_{0.89}Ti_{0.03})_{\Sigma = 2}$ O_4. The olivine crystals were too fine-grained (< 1 μm) to be analyzed using the microprobe (spot size: ~ 1 μm^2), but they were identified as forsteritic olivine by Raman spectrometry (Fig. 5). These minerals are embedded in a Mn- and P-enriched basaltic glass having a plagioclase-like chemical composition, given in Table 3. The IR spectra shown in Fig. 7, made on a bulk powder, confirm the pyroxene and olivine composition. As this basalt was produced from a dry, degassed melt, it does not contain any hydrous minerals (e.g., amphibole, clay). This sample is very similar to the samples produced by Faure et al. (2006) (see Figs. 14a and 14b in Faure et al. 2006).

Rapidly Cooled Basalt-Sample 11AR02

This drop-quenched sample shows a similar mineralogy and crystallization sequence to that of the slowly cooled basalt 11AR01. However, it is characterized by a different crystal size and texture (Fig. 3). Early spinels have a structural formula of $(Fe^{2+}{}_{0.65}Mg_{0.25})_{\Sigma = 1}$ $(Fe^{3+}{}_{1.67}Al_{0.23}Ti_{0.06})_{\Sigma = 2}$ O_4. They are Cr-free, Fe^{3+}-richer and Al-poorer than spinels formed in the more slowly cooled sample. They are surrounded by later, polyhedral olivine crystals, with a near-forsteritic chemical composition of $(Fe_{0.50}Mg_{1.50})_{\Sigma = 2}$ (SiO_4) with traces of

Table 3. Average chemical composition in weight percent of minerals and glass measured by electronic microprobe in the samples 11AR01 (slow cooling) and 11AR02 (drop-quenched) and associated 2σ error.

Oxides, wt%	K_2O	SiO_2	FeO	CaO	Na_2O	TiO_2	Al_2O_3	MnO	Cr_2O_3	MgO	NiO	P_2O_5	Total
11AR01													
Pyroxene	0.059	47.543	16.821	4.835	0.865	0.631	11.028	0.387	0.021	17.022	0.134	0.904	100.249
2σ	0.093	1.526	2.252	1.580	1.250	0.046	3.966	0.067	0.036	5.830	0.095	0.197	–
Spinel	0.006	1.294	42.586	0.261	0.061	1.069	17.240	0.289	21.815	9.599	0.484	0.053	94.755
2σ	0.013	1.446	0.857	0.127	0.052	0.080	3.399	0.065	2.928	0.795	0.134	0.043	–
Glass	0.330	50.633	11.519	8.180	3.988	0.708	18.574	0.230	0.016	3.392	0.005	1.579	99.153
2σ	0.034	1.612	0.652	1.338	0.360	0.161	1.472	0.094	0.025	1.833	0.013	0.278	–
11AR02													
Olivine	0.014	33.599	24.758	0.251	0.032	1.434	1.332	0.301	0.181	39.032	0.093	0.073	101.100
2σ	0.011	14.745	19.264	0.078	0.030	2.348	3.089	0.106	0.144	13.762	0.076	0.047	–
Spinel	0.009	0.137	73.114	0.058	0.049	3.613	6.208	0.330	0.065	7.268	0.000	0.024	90.873
2σ	0.004	0.012	4.601	0.028	0.041	1.762	1.292	0.053	0.092	0.483	0.000	0.008	–
Glass	0.212	46.438	15.888	7.225	2.914	1.706	13.555	0.285	0.135	9.927	0.009	0.299	98.594
2σ	0.054	6.068	2.118	2.669	0.760	1.055	4.892	0.104	0.296	6.950	0.015	0.111	–

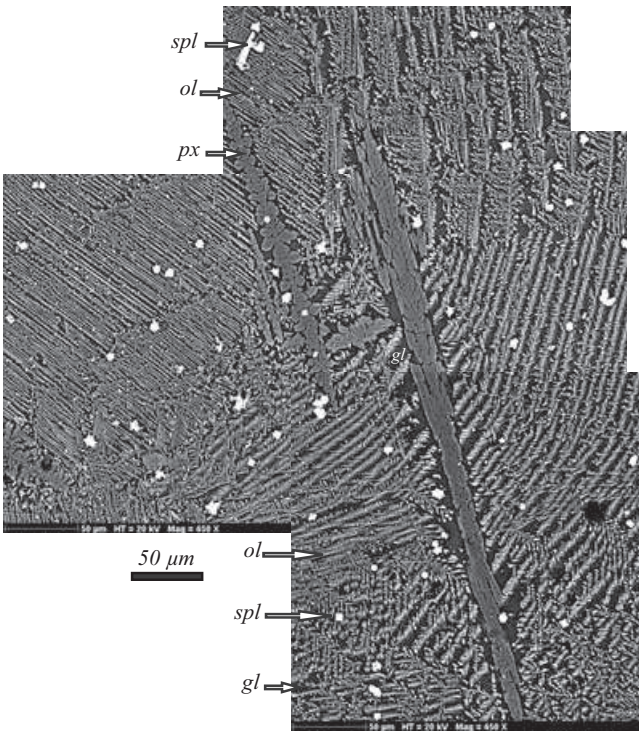

Fig. 4. SEM backscattered image of the inner part of 11AR01 sample (slowly cooled) at 20 kV and 10 nA. In light gray, the olivine (*ol*) with dentritic texture and in darker gray, the elongate pyroxene, calcic augite to Mg-pigeonite in composition (*px*), with the spinel grains (*spl*) in white and the basaltic glass in black (*gl*). Pyroxenes appear skeletal. Scale bar : 50 μm.

Ti and Al (Fo_{75}; Table 3). Based on their habits (see Fig. 3), they can interpreted as sub-liquidus olivines (Faure et al. 2007). Very fine skeletal to feathery dendritic pyroxene crystals were observed in a glass. These crystals were too small to be analyzed with the electron microprobe, but were revealed by Raman spectroscopy. The glassy matrix predominates in this basalt compared with the slowly cooled sample 11AR01. Its chemical composition in weight oxide percent is given in Table 3. The glass is not enriched in P_2O_5 and we presume that this component was segregated in the pyroxenes crystals.

DISCUSSION

Komatiites on Mars?

In this study, we prepared two Fe- Mg-rich basalts, chemically similar to Martian basalts from the Gusev crater with compositions corrected for alteration at the surface of Mars on rocks examined by Spirit (cf. McSween et al. 2009). Rock compositions in Gusev crater, however, may not be representative of the whole Martian surface.

There are some differences between our artificial basalts and those on Mars. Compared with the ten Gusev basalts ranging from unaltered to slightly altered that were chosen as the baseline for this study, the silica (SiO_2) composition in our basalts is slightly lower than the very fresh basalts (Adirondack, Humphrey, and Mazatzal Brooklyn). However, the high Fe and Mg contents are similar. Some basalts observed on Mars contain euhedral olivine (McSween et al. 2004), whereas olivines in our samples are either small and acicular (slow cooling 11AR01) or quasi-euhedral (drop-quenched basalt-11AR02). The absence of plagioclase feldspar in these samples is due to the low Ca and Al-content compensated by high Mg and Fe-content, a phenomenon already known in primitive melts. One of the interesting results from our study is that the more slowly cooled basalt has textures and mineralogies

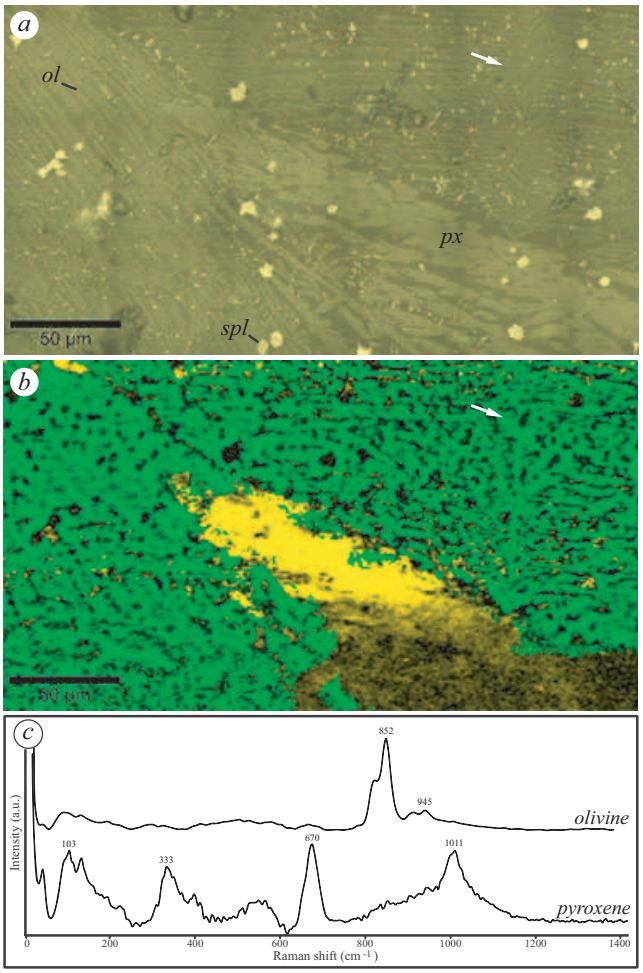

Fig. 5. 11AR01 (slowly cooled sample). a) Reflected light optical view showing large elongate augitic crystals (*px*), dentritic crystals forsterite (*ol*, *white arrow*), and small spinels (*spl*). b) Raman mapping of (a); augite is in yellow and forsterite in green, and the spinels do not give any spectrum. Forsterite composition is indicated by Raman measurements only because the crystals are too small to be measured by microprobe. c) Raman spectra used for mapping (analytical conditions: laser power ~10 mW; obj. × 100).

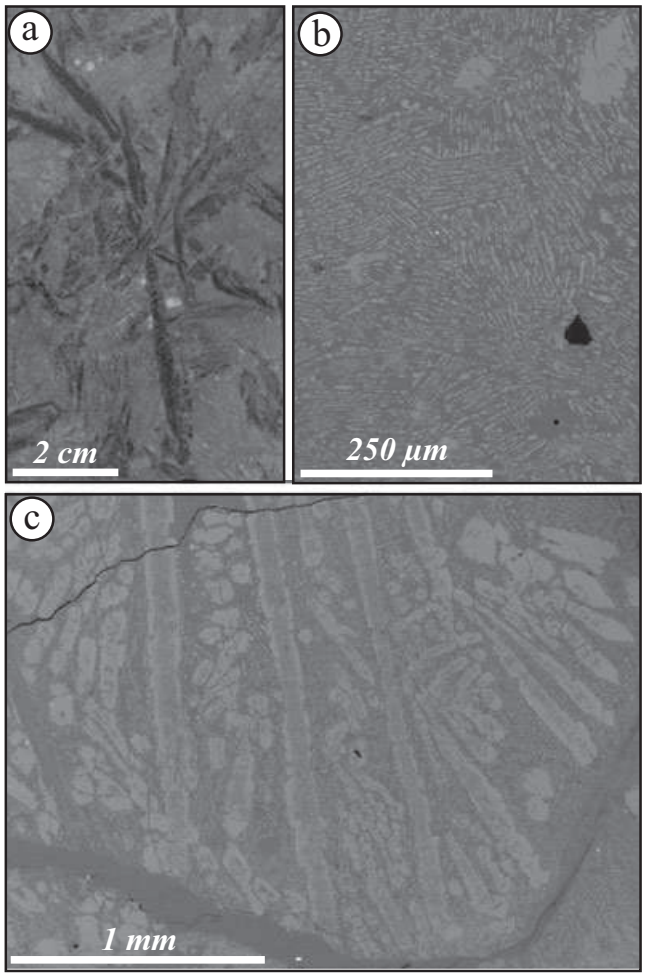

Fig. 6. Terrestrial komatiite sample from Dundonald: a) macroscopic image; b), c) backscattered images showing spinifex textures. The texture of sample 11AR01 (Fig. 3, 4) is very similar to this texture.

similar to terrestrial komatiites (Fig. 4 and 6). These rocks were very common on the early Earth during the Archaean epoch, which corresponds to the Noachian on Mars. They are Mg-rich rocks produced by very thin, fluid lavas extruded at the surface (and not at depth in the ocean). Indeed, it has been suggested that komatiites could be present on Mars (Reyes and Christensen 1994; Nna-Mvondo and Martinez-Frias 2007). There is evidence of very fluid lava flows in Gusev crater and on Tharsis (e.g., Greeley et al. 2005 and Mangold et al. 2009), comparable to komatiite lava flows on the early Earth. However, to date, spinifex textures have not yet been observed by the MI imager on the Spirit and Opportunity MERs, perhaps because of the rapid alteration of these kinds of rocks. Our study, however, supports the suggestion that spinifex-textured basaltic rocks (similar to 11AR01) or true komatiites could occur on Mars. Although komatiites have a higher Mg-content than the basalts in this study (Mg ~12 wt%), we suggest that the lower Mg-content could be compensated by a high content of Fe. Our samples contain 29.90 wt% of MgO + FeO, which is similar to an average composition of a Barberton-type komatiite (30 wt% of MgO + FeO; Arndt 2003).

Comparison with Previous Studies

Our synthetic basalts are different from those previously produced by Tosca et al. (2004) and Hurowitz et al. (2005) because both melt compositions and experimental P-T melting conditions were different. The synthesis pressure conditions used by Tosca et al.

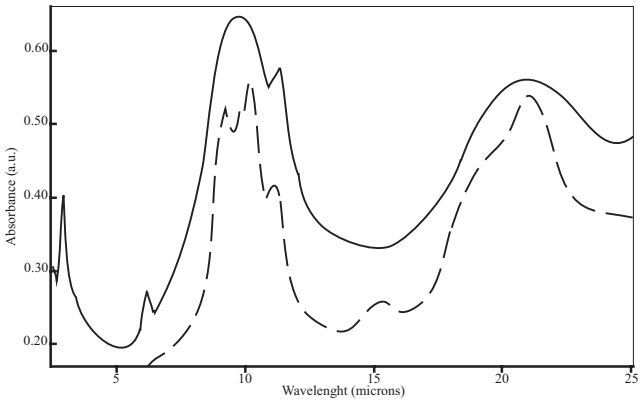

Fig. 7. IR spectrum in absorbance of 11AR01. Pyroxene is identified by its spectrum (dotted line) by comparison with data base of the Research Branch of Agriculture in Canada.

(2004) are comparable to ours, $\sim 10^5$ Pa, but we used 1350 °C, whereas these authors used ~1120 °C. The chemical composition of the melt thus produced from the Pathfinder soil by Tosca et al. (2004) was close to the melt we produced, but was different from the silica-rich Pathfinder rock (Fig. 1). Moreover, because Tosca et al. (2004) immediately ground their sample to a powder for the alteration experiment, it is not possible to compare their mineralogy and texture with those of our synthetic basalts. The artificial rock produced by Hurowitz et al. (2005) was obtained at ~1135 °C and at ~0.1 Pa (~1 mbar). The rock was cooled very slowly (~6 °C h^{-1}) and a "holocrystalline basalt with aphanitic-porphyritic texture" without glass was produced, a texture which is more similar to a gabbro than to a basalt. A further difference is that the chemical composition of the melt synthesized by Hurowitz et al. (2005) was a shergottite analog of the Los Angeles meteorite which, with its very low Mg-content, of being is different from the basaltic rocks from the Gusev crater on Mars (Fig. 1b).

Implications for Early Life on Mars

The volcanics in Gusev crater are of Noachian age (Soderblom and Bell 2008). This is the period when Mars had somewhat similar environmental conditions to those of the early Earth and was potentially habitable (Westall 2005; Bibring et al. 2006; Jakosky et al. 2007; Southam et al. 2007; Westall et al. 2011). As noted above, Fe-Mg-rich basalts and komatiite-type basalts were common on the early Earth. Such rocks are favored habitats for chemolithotrophic microorganisms that obtain their energy and nutrients from them (cf. Furnes et al. 2007). Furthermore, alteration of these rocks would have produced Fe-Mg clays, such as nontronite and chlorite-saponite, that could have been implicated in the concentration of prebiotic organics and, thus, in various scenarios for the origin of life (Meunier et al. 2010). Given the interpretations of such materials associated with Noachian terranes on the surface of Mars (Poulet et al. 2005; Bibring et al. 2006; Mustard et al. 2008; Ehlmann et al. 2009), we can extend the analogy with the early Earth to hypothesize the potential importance of these kinds of rocks and their alteration products for not only an origin of Martian life, but also as habitats for Martian microorganisms. Both samples could be weathered by glass alteration. The drop-quenched sample contains more glass and would be rapidly altered, whereas the spinifex texture could be a site of preferential development of clays (such as nontronite) along specific surfaces (elongates grain surfaces). This could favor the colonization of volcanic rocks by microorganisms, in particular chemolithotrophs. For example, traces of the activities of such organisms have been preserved in basalts and derivatives of volcanic rocks from the Early Archaean terranes of Barberton and the Pilbara (review in Westall et al. 2006; Furnes et al. 2007; Westall et al. 2011) as well as in amygdules in pillow basalts (Cavalazzi et al. 2011). Moreover, typical alteration of the mafic rocks, such as komatiites, in aqueous conditions, a high pH, and low $aSi0_2$ leads to serpentinization. (This reaction produces H_2, which can serve as an important energy source for chemosynthetic organisms [Schulte et al. 2006].) Note that biological activity is associated with serpentinization processes in hydrated mantle (Ménez et al. 2012). Furthermore, serpentine deposits have been observed on the Martian surface (Ehlmann et al. 2010) and could be a possible habitat for early life on Mars. Thus, if life ever appeared on Mars, it is possible that traces of its existence could be found directly in the surfaces, cracks, and vesicles of these volcanic rock types. In situ missions to Mars should examine such rocks if there is evidence that they have been associated with water.

CONCLUSION

We have produced experimental Fe-Mg-rich basalts with compositions based on the geochemical data from Gusev basalts on Mars to obtain relevant analog samples for the International Space Rockstore (ISAR; www.isar.cnrs-orleans.fr). One slowly cooled (one day, ~110 °C h^{-1}) synthetic basalt presents specific spinifex textures that are very similar to those of early Earth basalts and komatiites that were formed in an equivalent period to the Noachian and Hesperian on Mars. Fe-Mg-rich basalts and their alteration products are also highly relevant for the appearance and habitability of life. Nontronite and chloritic clays could have concentrated prebiotic organic molecules that were the building bricks of life, whereas surfaces, cracks, and vesicles in such

lavas were ideal habitats for primitive anaerobic life forms, such as chemolithotrophic microorganisms (Furnes et al. 2007; Cavalazzi et al. 2011). Our basalts therefore represent an important addition to the ISAR collection for testing space flight instrumentation.

Acknowledgments——This work was supported by CNES (Centre National d'Etudes Spatiales) and the Region Centre. We acknowledge Sabine Petit, Alain Meunier, and Ida Di Carlo for assistance in the IR measurements and the electronic microprobe data, respectively. We acknowledge Sylvio Rotolo for providing the Etna volcanic sample (Table 2). FG is supported by the ERC-contract 279790.

Editorial Handling——Dr. Gordon Osinski

REFERENCES

Arndt N. T. 2003. Komatiites, kimberlites, and boninites. *Journal of Geophysical Research* 108:B6–2293, doi:10.1029/2002JB00215.

Arndt N. T., Lesher C. M., Houlé M. C., Lewin E., and Lacaze Y. 2004. Intrusion and crystallization of a spinifex-textured komatiite sill in Dundonald Township, Ontario. *Journal of Petrology* 45:2555–2571.

Bibring J.-P., Langevin Y., Mustard J. F., Poulet F., Arvidson R., Gendrin A., Gondet B., Mangold N., Pinet P., Forget F., and the OMEGA Team. 2006. Global mineralogical and aqueous mars history derived from OMEGA/Mars Express data. *Science* 312:400–404. doi: 10.1126/science.1122659.

Bost N., Westall F., Ramboz C., Foucher F., Pullan D., Meunier A., Petit S., Fleischer I., Klingelhöfer G., and Vago J. L. 2011. **2018 MAX-C/ExoMars mission: The Orleans Mars-analogue rock collection for instrument testing**. (abstract #1347). 42nd Lunar and Planetary Science Conference. CD-ROM.

Bryan W. B. 1972. Morphology of quench crystals in submarine basalts. *Journal of Geophysical Research* 77:5812–5819.

Cavalazzi B., Westall F., Cady S. L., Barbieri R., and Foucher F. 2011. Potential fossil endoliths in vesicular pillow basalt, Coral Patch Seamount, eastern North Atlantic Ocean. *Astrobiology* 11:619–632.

Economou T. E. 2001. Chemical analyses of Martian soil and rocks obtained by the Pathfinder Alpha Proton X-ray Spectrometer. *Radiation Physics and Chemistry* 61:191–197.

Ehlmann B. L., Mustard J. F., Swayze G. A., Clark R. N., Bishop J. L., Poulet F., Des Marais D. J., Roach L. H., Milliken R. E., Wray J. J., Barnouin-Jha O., and Murchie S. 2009. Identification of hydrated silicate minerals on Mars using MRO-CRISM: Geologic context near Nili Fossae and implications for aqueous alteration. *Journal of Geophysical Research* 114:E00D08. doi:10.1029/2009JE003339.

Ehlmann B. L., Mustard J. F., and Murchie S. L. 2010. Geologic setting of serpentine depostis on Mars. *Geophysical Research Letters* 37:L06201. doi:10.1029/2010GL042596.

Faure F., Arndt N., and Libourel G. 2006. Formation of spinifex texture in komatiites: An experimental study. *Journal of Petrology* 47:1591–1610. doi:10.1093/petrology/egl1021.

Faure F., Schiano P., Trolliard G., Nicollet C., and Soulestin B. 2007. Textural evolution of polyhedral olivine experiencing rapid cooling rates. *Contribution to Mineralogy and Petrology* 153:405–416.

Filiberto J., Treiman A. H., and Le L. 2008. Crystallization experiments on a Gusev Adirondack basalt composition. *Meteoritics* 43:1137–1146.

Furnes H., Banerjee N. R., Staudigel H., Muehlenbachs K., McLoughlin N., de Wit M., and Van Kranendonk M. 2007. Comparing petrographic signatures of bioalteration in recent to Mesoarchean pillow lavas: Tracing subsurface life in oceanic igneous rocks. *Precambrian Research* 158:156–176. doi:10.1016/j.precamres.2007.04.012.

Gaillard F. and Scaillet B. 2009. The sulfur content of volcanic gases on Mars. *Earth and Planetary Science Letters* 279: 34–43.

Gaillard F., Pichavant M., and Scaillet B. 2003. Experimental determination of activities of FeO and Fe_2O_3 components in hydrous silica melts under oxidizing conditions. *Geochimica et Cosmochimica Acta* 67:4389–4409.

Gellert R., Rieder R., Brückner J., Clark B. C., Dreibus G., Klingelhöfer G., Lugmair G., Ming D. W., Wänke H., Yen A., Zipfel J., and Squyres S. W. 2006. Alpha particle X-ray spectrometer (APXS): Results from Gusev crater and calibration report. *Journal of Geophysical Research* 111:E02S05. doi:10.1029/2005JE002555.

Greeley R., Foing B. H., McSween H. Y., Neukum G., Pinet P., van Kan M., Werner S. C., Williams D. A., and Zegers T. E. 2005. Fluid lava flows in Gusev crater, Mars. *Journal of Geophysical Research* 110:E05008. doi:10.1029/2005JE002401.

Greenberger R. N., Mustard J. F., Kumar P. S., Dyar M. D., Speicher E. A., and Skulte E. C. 2011. Weathering products of Deccan basalts and implications for Mars (abstract #2548). 42nd Lunar and Planetary Science Conference. CD-ROM.

Halevy I., Zuber M. T., and Schrag D. P. 2007. A sulfur dioxide climate feedback on early Mars. *Science* 318:1903–1907. doi: 10.1126/science.1147039.

Herd C. D. K. 2006. Insights into the redox history of the NWA 1068/1110 Martian basalt from mineral equilibria and vanadium oxybarometry. *American Mineralogist* 91:1616–1627. doi:10.2138/am.2006.2104.

Herd C. D. K., Borg L. E., Jones J. H., and Papike J. J. 2002. Oxygen fugacity and geochemical variations in the Martian basalts: Implications for Martian basalt petrogenesis and the oxidation state of the upper mantle of Mars. *Geochimica et Cosmochimica Acta* 66:2025–2036.

Hurowitz J. A., McLennan S. C., Lindsley D. H., and Schoonen M. A. 2005. Experimental epithermal alteration of synthetic Los Angeles meteorite: Implication for the origin of Martian soils and identification of hydrothermal sites on Mars. *Journal of Geophysical Research* 110:E07002. doi:10.1029/2004JE002391.

Hurowitz J. A., McLennan S. M., Tosca N. J., Arvidson R. E., Michalski J. R., Ming D. W., Schröder C., and Squyres S. W. 2006. In situ and experimental evidence for acidic weathering of rocks and soils on Mars. *Journal of Geophysical Research* 111:E02S19. doi:10.1029/2005JE002515.

Jakosky B. M., Westall F., and Brack A. 2007. Mars. In *Planets and life: The emerging science of astrobiology*, edited

by Sullivan W. T., and Baross J. A. Cambridge: Cambridge University Press. pp. 357–387.

Le Bas M. J. 2000. IUGS reclassification of the high-Mg and picritic volcanic rocks. *Journal of Petrology* 41:1467–1470.

Mangold N., Loizeau D., Poulet F., Ansan V., Baratoux D., LeMouelic S., Bardintzeff J.-M., Platevoet B., Toplis M., Pinet P., Masson P., Bibring J.-P., Gondet B., Langevin Y., and Neukum G. 2009. Mineralogy of recent volcanic plains in the Tharsis region, Mars, and implications for platy-ridged flow composition. *Earth and Planetary Science Letters* 294:440–450. doi:10.1016/j.epsl.2009.07.36.

McAdam A. C., Zolotov M. Y., Sharp T. G., and Leshin L. A. 2008. Preferential low-pH dissolution of pyroxene in plagioclase-pyroxene mixtures: Implication for Martian surface materials. *Icarus* 196:90–96. doi:10.1016/j.icarus.2008.01.008.

McSween H. Y., Arvidson R. E., Bell J. F. III, Blaney D., Cabrol N. A., Christensen P. R., Clark B. C, Crisp J. A., Crumpler L. S., Des Marais D. J., Farmer J. D., Gellert R., Ghosh A., Gorevan S., Graff T., Grant J., Haskin L. A., Herkenhoff K. E., Johnson J. R., Jolliff B. L., Klingelhoefer G., Knudson A. T., McLennan S., Milam K. A., Moersch J. E., Morris R. V., Rieder R., Ruff S. W., de Souza P. A., Squyres S. W., Wänke H., Wang A., Wyatt M. B., Yen A., and Zipfel J. 2004. Basaltic rocks analyzed by the Spirit Rover in Gusev crater. *Science* 305:842–845. doi:10.1126/science.3050842.

McSween H. Y., Taylor G. J., and Wyatt M. B. 2009. Elemental composition of the Martian crust. *Science* 324:736–739. doi: 10.1126/science.1165871.

Ménez B., Pasini V., and Brunelli D. 2012. Life in the hydrated suboceanis mantle. *Nature Geoscience* 5:133–137. doi:10.1038/NGEO1359.

Meunier A., Petit S., Cockell C. S., El Albani A., and Beaufort D. 2010. The Fe-rich clay microsystems in basalt-komatiite lavas: Importance of Fe-smectites for pre-biotic molecules catalysis during the Adean eon. *Origins of Life and Evolution of Biospheres* 40:253–272. doi:10.1007/s11084-010-9205-2.

Ming D. W., Gellert R., Morris R. V., Arvidson R. E., Brückner J., Clark B. C., Cohen B. A., d'Uston C., Economou T., Fleischer I., Klingelhöfer G., McCoy T. J., Mittlefehldt D. W., Schmidt M. E., Schröder C., Squyres S. W., Tréguier E., Yen A. S., and Zipfel J. 2008. Geochemical properties of rocks and soils in Gusev crater, Mars: Results of the Alpha Particle X-Ray Spectrometer from Cumberland Ridge to Home Plate. *Journal of Geophysical Research* 113:E12S39. doi:10.1029/2008JE003195.

Monders A. G., Médard E., and Grove T. L. 2007. Phase equilibrium investigations of the Adirondack class basalts from the Gusev plains, Gusev crater, Mars. *Meteoritics & Planetary Science* 42:131–148.

Morris R. V., Klingelhöfer G., Schröder C., Rodionov D. S., Yen A., Ming D. W., de Souza P. A. Jr., Fleischer I., Wdowiak T., Gellert R., Bernhardt B., Evlanov E. N., Zubkov B., Foh J., Bonnes U., Kankeleit E., Gütlich P., Renz F., Squyres S. W., and Arvidson R. E. 2006. Mössbauer mineralogy of rock, soil, and dust at Gusev crater, Mars: Spirit's journey through weakly altered olivine basalt on the plains and pervasively altered in the Columbia Hills. *Journal of Geophysical Research* 111: E02S13. doi:10.1029/2005JE002584.

Musselwhite D. S., Dalton H. A., Kiefer W. S., and Treiman A. H. 2006. Experimental petrology of the basaltic shergottites Yamato-980459: Implications for the structure of the Martian mantle. *Meteoritics & Planetary Science* 41:1271–1290.

Mustard J. F., Murchie S. L., Pelkey S. M., Ehlmann B. L., Milliken R. E., Grant J. A., Bibring J.-P., Poulet F., Bishop J., Noe Dobrea E., Roach L., Seelos F., Arvidson R. E., Wiseman S., Green R., Hash C., Humm D., Malaret E., McGovern J. A., Seelos K., Clancy T., Clark R., Marais D. D., Izenberg N., Knudson A., Langevin Y., Martin T., McGuire P., Morris R., Robinson M., Roush T., Smith M., Swayze G., Taylor H., Titus T., and Wolff M. 2008. Hydrated silicate minerals on Mars observed by the Mars Reconnaissance Orbiter CRISM instrument. *Nature* 454:305–309. doi:10.1038/nature07097.

Nesbit H. W. and Wilson R. E. 1992. Recent chemical weathering of basalts. *American Journal of Science* 292:740–777.

Nna-Mvondo D. and Martinez-Frias J. 2007. Review komatiites: From Earth's geological settings to planetary and astrobiological contexts. *Earth, Moon, and Planets* 100:157–179.

Pommier A., Gaillard F., and Pichavant M. 2010. Time-dependent changes of the electrical conductivity of basaltic melts with redox state. *Geochimica et Cosmochimica Acta* 74:1653–1671.

Poulet F., Bibring J.-P., Mustard J. F., Gendrin A., Mangold N., Langevin Y., Arvidson R. E., Gondet B., Gomez C., and the Omega Team. 2005. Phyllosilicates on Mars and implications for early Martian climate. *Nature* 438:623–627. doi:10.1038/nature04274.

Reyes D. P. and Christensen P. R. 1994. Evidence for komatiite-type lavas on Mars from Phobos ISM data and other observations. *Geophysical Research Letters* 21:887–890.

Rieder R., Gellert R., Anderson R. C., Brückner J., Clark B. C., Dreibus G., Economou T., Klingelhöfer G., Lugmair G. W., Ming D. W., Squyres S. W., d'Uston C., Wänke H., Yen A., and Zipfel J. 2004. Chemistry of rocks and soils at Meridiani Planum from the Alpha Particles X-Ray Spectrometer. *Science* 306:1746–1749. doi: 10.1126/science.1104358.

Rubin A., Warren P., Greenwood J., Verish R., Leshin L., Hervig R., Clayton R., and Mayeda T. 2000. Los Angeles: The most differentiated basaltic Martian meteorite. *Geology* 28:1011–1015.

Schmidt M. E., Schrader C. M., and McCoy T. J. 2011. How oxidized are the Gusev basalts? (abstract #2277). 42nd Lunar and Planetary Science Conference. CD-ROM.

Schulte M., Blake D., Hoehler T., and McCollom T. 2006. Serpentinization and its implications for life on the early Earth and Mars. *Astrobiology* 6:364–376. doi:10.1089/ast.2006.6.364.

Soderblom L. A. and Bell J. F. 2008. Exploration of the Martian surface: 1992–2007. In *The Martian surface: Composition, mineralogy, and physical properties*, edited by Bell J. F. III. Cambridge: Cambridge University Press. pp. 3–19.

Southam G., Rothschild L. J., and Westall F. 2007. The geology and habitability of terrestrial planets: Fundamental requirements for life. *Space Science Review* 129:7–34.

Squyres S. W., Arvidson R. E., Bell J. F. III, Brückner J., Cabrol N. A., Calvin W., Carr M. H., Christensen P. R., Clark B. C., Crumpler L., Des Marais D. J., d'Uston C., Economou T., Farmer J., Farrand W., Folkner W., Golombek M., Gorevan S., Grant J. A., Greeley R.,

Grotzinger J., Haskin L., Herkenhoff K. E., Hviid S., Johnson J., Klingelhöfer G., Knoll A., Landis G., Lemmon M., Li R., Madsen M. B., Malin M. C., McLennan S. M., McSween H. Y., Ming D. W., Moersch J., Morris R. V., Parker T., Rice Jr . J. W., Richter L., Rieder R., Sims M., Smith M., Smith P., Soderblom L. A., Sullivan R., Wänke H., Wdowiak T., Wolff M., and Yen A. 2004. The Spirit rover's Athena science investigation at Gusev crater, Mars. *Science* 305:794–799. doi: 10.1126/science.3050794.

Stanley B. D., Hirschmann M. M., and Withers A. C. 2011. CO_2 solubility in Martian basalts and Martian atmospheric evolution. *Geochimica et Cosmochimica Acta* 75:5987–6003. doi:10.1016/j.gca.2011.07.027.

Tosca N. J., McLennan S. M., Lindsley D. H., and Schoonen M. A. A. 2004. Acid-sulfate weathering of synthetic Martian basalt: The acid fog model revisited. *Journal of Geophysical Research* 109:E05003. doi:10.1029/2003JE002218.

Viles H., Ehlmann B., Wilson C. F., Cebula T., Page M., and Bourke M. 2010. Simulating weathering of basalt on Mars and Earth by thermal cycling. *Geophysical Research Letters* 37:L18201. doi: 10.1029/2010GL043522.

Wänke H. J., Bruckner G., Dreibus R., Rieder R., and Ryabchikov I. 2001. Chemical composition of rocks at the Pathfinder site. *Space Science Reviews* 96:317–330.

Westall F. 2005. Early life on Earth and analogies to Mars. In *Water on Mars and life: Advances in astrobiology and biogeophysics*, edited by Tokano T. Berlin, Heidelberg: Springer. pp. 45–64. doi: 10.1007/b12040.

Westall F., de Vries S. T., Nijman W., Rouchon V., Orberger B., Pearson V., Watson J., Verchovsky A., Wright I., Rouzaud J. N., Marchesini D., and Anne S. 2006. The 3.466 Ga "Kitty's Gap Cheil," an early Archean microbial ecosystem. South Africa Processes On The Early Earth, Field Forum on Processes on the Early Earth 405:105–131.

Westall F., Foucher F., Cavalazzi B., de Vries S. T., Nijman W., Pearson V., Watson J., Verchovsky A., Wright I., Rouzaud J.-N., Marchesini D., and Anne S. 2011. Volcaniclastic habitats for early life on Earth and Mars: A case study from $\sim$ 3.5 Ga-old rocks from the Pilbara Australia. *Planetary and Space Science* 59:1093–1106. doi:10.1016/j.pss.2010.09.006.

Zipfel J., Anderson R., Brückner J., Clark B. C., Dreibus G., Economou T., Gellert R., Klingelhöfer G., Lugmair G. W., Ming D., Reider R., Squyres S. W., d'Uston C., Wänke H, and Yen A. 2004. APXS analyses of bounce rock — The first shergottites on Mars. *Meteoritics & Planetary Science* 39 (Suppl): A118.